The Journal of Experimental Biology 204, 3425–3441 (2001)
Printed in Great Britain © The Company of Biologists Limited 2001
JEB3379

Benefits of haemoglobin in the cladoceran crustacean *Daphnia magna*

R. Pirow*, C. Bäumer and R. J. Paul

Institut für Zoophysiologie, Westfälische Wilhelms-Universität, Hindenburgplatz 55, D-48143 Münster, Germany

*e-mail: pirow@uni-muenster.de

Accepted 24 July 2001

Summary

To determine the contribution of haemoglobin (Hb) to the hypoxia-tolerance of *Daphnia magna*, we exposed Hb-poor and Hb-rich individuals (2.4–2.8 mm long) to a stepwise decrease in ambient oxygen partial pressure (P_{O_2amb}) over a period of 51 min from normoxia (20.56 kPa) to anoxia (<0.27 kPa) and looked for differences in their physiological performance. The haem-based concentrations of Hb in the haemolymph were 49 μmol l^{-1} in Hb-poor and 337 μmol l^{-1} in Hb-rich animals, respectively. The experimental apparatus made simultaneous measurement of appendage beating rate (f_A), NADH fluorescence intensity (I_{NADH}) of the appendage muscles, heart rate (f_H) and *in vivo* Hb oxygen-saturation possible. In response to progressive, moderate hypoxia, both groups showed pronounced tachycardia and a slight decrease in f_A. The f_A and f_H of Hb-rich animals were generally 4–6 % lower than those of Hb-poor animals. In addition, Hb-rich animals showed a significant decrease in the P_{O_2amb} at which the Hb in the heart region was half-saturated and a striking reduction in the critical P_{O_2amb} of appendage-related variables. In Hb-poor animals, the I_{NADH} signal indicated that the oxygen supply to the limb muscle tissue started to become impeded at a critical P_{O_2amb} of 4.75 kPa, although the high level of f_A was largely maintained until 1.77 kPa. The obvious discrepancy between these two critical P_{O_2amb} values suggested an anaerobic supplementation of energy provision in the range 4.75–1.77 kPa. The fact that I_{NADH} of Hb-rich animals did not rise until P_{O_2amb} fell below 1.32 kPa strongly suggests that the extra Hb available to Hb-rich animals ensured an adequate oxygen supply to the limb muscle tissue in the P_{O_2amb} range 4.75–1.32 kPa. This finding illustrates the physiological benefit of Hb in enabling the animal to sustain its aerobic metabolism as the energetically most efficient mode of fuel utilization under conditions of reduced oxygen availability.

Key words: Crustacea, Branchiopoda, Cladocera, *Daphnia magna*, zooplankton, haemoglobin, oxygen transport, ventilatory system, circulatory system, respiration, NADH.

Introduction

Haemoglobin (Hb) plays a vital role in many advanced organisms in forming a constitutive part of their oxygen-transport systems. Almost all vertebrates require a constantly high concentration of this oxygen carrier in the circulatory fluid (Prosser and Brown, 1961), and any lack or functional failure would have lethal consequences. Within the invertebrates, Hb occurs sporadically in various phyla (Terwilliger, 1980; Vinogradov, 1985; Terwilliger, 1998), and the concentration in the body fluids is usually lower than in vertebrates (Prosser and Brown, 1961) and can vary greatly depending on environmental conditions (Fox, 1955; Weber, 1980; Terwilliger, 1998). The effects of the environment on the control of Hb synthesis are especially pronounced in aquatic invertebrates such as the Cladocera. These small-sized crustaceans, which often represent the dominant constituent of freshwater zooplankton communities (Brönmark and Hansson, 1998), show a strong induction of Hb synthesis in response to environmental hypoxia (Fox et al., 1951; Fox, 1955; Kobayashi and Hoshi, 1982). Although this response improves the tolerance of hypoxic conditions (Fox et al., 1951), it can also have other more ambivalent consequences. The costs and benefits have to be taken into account as well as alternative strategies to cope with hypoxia.

For example, evading oxygen-poor microhabitats (Sell, 1998) or enduring short-term periods of oxygen deficiency by means of anaerobic metabolism (Usuki and Yamagushi, 1979; Paul et al., 1998) represent two possible solutions that can make the oxygen carrier dispensible. However, planktonic filter feeders such as those of the genus *Daphnia* are highly competitive species that can derive a significant ecological advantage when attaining the physiological competence to graze, for instance, in a nutrient-rich but oxygen-poor metalimnion (Williamson et al., 1996; Sell, 1998) while sustaining aerobic energy transformation. In addition, hypoxic deep waters can also function as a refuge from predation (Lampert, 1989; Lampert, 1993). Predator avoidance or access to alternative food resources, combined with efficient fuel utilization largely independent from fluctuations in oxygen availability, promote survival, growth and reproduction and result in higher fitness.

The benefits derived from Hb become, however, diminished by two cost factors. The synthesis of Hb decreases the amount of matter and energy that can be invested into growth and reproduction (Fox et al., 1951; Green, 1955; Kobayashi, 1982; Kobayashi and Hoshi, 1984). Moreover, an increased Hb content in the haemolymph results in a reddish coloration and can make these transparent animals more conspicuous to visually foraging predators (Vinyard and O'Brien, 1975; Confer et al., 1978; O'Brien, 1979). A 'prophylactic' elevation of Hb concentration that imparts a higher tolerance towards environmental hypoxia is therefore not always the optimum solution in terms of ecological fitness.

These conflicting circumstances certainly explain the interspecific, interclonal, inter- and intraindividual variability in Hb concentration (Fox, 1948; Fox et al., 1949; Green, 1956; Carvalho, 1984; Weider, 1985; Weider and Lampert, 1985) as well as the sensitive environmental control of Hb expression. For *Daphnia magna*, a euryoxic species that naturally occupies eutrophic ponds and ditches (Flößner, 1972), Tokishita et al. (Tokishita et al., 1997) reported a more than tenfold elevation in levels of a Hb mRNA when animals were reared under oxygen-poor conditions. Similarly, Kobayashi and Hoshi (Kobayashi and Hoshi, 1982) found a 16-fold increase in the haemolymph Hb concentration. This physiological adaptation, however, is more complex than simply synthesizing more Hb. Instead, the oxygen-affinity of Hb increases as a result of an altered subunit composition of the multimeric protein (Kobayashi et al., 1988), indicating that other Hb genes are preferentially expressed under these conditions (Kimura et al., 1999). Recent studies have revealed that at least four Hb genes exist (Tokishita et al., 1997; Kimura et al., 1999; Hebert et al., 1999) which code for different subunits and give rise to multiple Hb species with different oxygen-binding affinities. This remarkable flexibility in adjusting both the quantity and quality of Hb raises the question of how Hb affects the physiological performance of the organism.

The principal function of Hb is beyond doubt. As a carrier that reversibly binds oxygen, Hb contributes to the transport of oxygen in the haemolymph. This can be deduced from hypoxic exposure experiments (Fox et al., 1951; Kring and O'Brien, 1976; Kobayashi and Gonoi, 1985), which have shown for various daphniid species that an increased Hb concentration in the haemolymph lowers the critical oxygen partial pressure below which filtering activity, swimming behaviour, oxygen consumption, reproduction and survivorship become severely impeded. The impairment of filtering activity seems to be the initial event that entails this spectrum of immediate and long-term effects. This is not particularly surprising as the persistent agitation of the thoracic limbs is of vital importance for both filter feeding and gas exchange (Fryer, 1991; Pirow et al., 1999a). The ability to sustain this activity under conditions of reduced oxygen availability represents, therefore, a suitable marker for the evaluation of the effects of Hb.

In the present study, we have attempted a detailed analysis of the physiological role of Hb in the water flea *Daphnia magna*. To determine the relative contribution of Hb to the hypoxia-tolerance of the organism, we exposed parthenogenetic Hb-poor and Hb-rich animals to a gradual transition from normoxia to anoxia and looked for differences in their physiological performance. Of the set of physiological variables measured, limb-beating activity was considered to be the key indicator for the evaluation of Hb-derived effects. Monitoring heart rate and the NADH fluorescence intensity of the appendage muscles, the latter as a marker of the tissue oxygenation state (Chance, 1991), allowed us to determine whether a low Hb concentration, and consequently a shortage of oxygen in the haemolymph, was counteracted in Hb-poor animals by circulatory adjustments or by processes of anaerobic energy provision. Finally, the determination of Hb concentration combined with an analysis of the *in vivo* oxygen-saturation of Hb made it possible to demonstrate the relationship between the haemolymph oxygen content and the ability to sustain limb-beating activity.

Materials and methods

Animals

Water fleas, *Daphnia magna* Straus, were originally obtained from the Staatliches Umweltamt, Nordrhein-Westfalen, Münster, Germany. The animals were kept in 2 l glass beakers at room temperature (19–22 °C) under a 16 h:8 h L:D photoperiod using daylight fluorescent lamps. The culture medium (M4; Elendt and Bias, 1990) had a pH of approximately 8.2 (19.3 °C), a salinity of 0.2 ‰ and a conductivity of 810 $\mu S\,cm^{-1}$ (19.3 °C; LF 196, WTW, Weilheim, Germany). The animals were fed with yeast and algae (*Scenedesmus subspicatus*) once daily.

Ten days before the start of the experiments, juvenile parthenogenetic offspring 1.5–1.8 mm in length were allocated to two groups and raised under normoxic (80–95 % air saturation, 19.5–21.5 °C) and hypoxic (8–10 % air saturation, 21.0–23.0 °C) conditions, respectively. For hypoxic incubation, batches of 25–30 animals were kept in 3 l preserving jars filled with 2.5 l of medium containing an additional 20 $mmol\,l^{-1}$ Fe^{2+}. The addition of extra ferrous iron has been reported to boost the formation of haemoglobin under hypoxic conditions (Fox and Phear, 1953; Kobayashi, 1981). The low oxygen partial pressure was achieved by reducing the atmospheric pressure in the residual air space of the preserving jar to 15.2 kPa using a vacuum pump (PC 511, Vacuubrand, Wertheim, Germany). The air saturation in the medium decreased gradually and reached the final level 4 days after the start of the incubation.

Normoxic (Hb-poor) animals were reared under the light conditions described above, whereas hypoxic (Hb-rich) animals were kept under continuous, dimmed light conditions. Dimmed light was empirically found to result in a stronger reddish coloration of the animals, indicating a higher haemoglobin concentration in the haemolymph. To exclude interference with yeast haemoglobin, both groups were fed only with algae (*Scenedesmus subspicatus*). Hypoxic animals were fed to excess, thus ensuring that food availability did not become an additional stress factor.

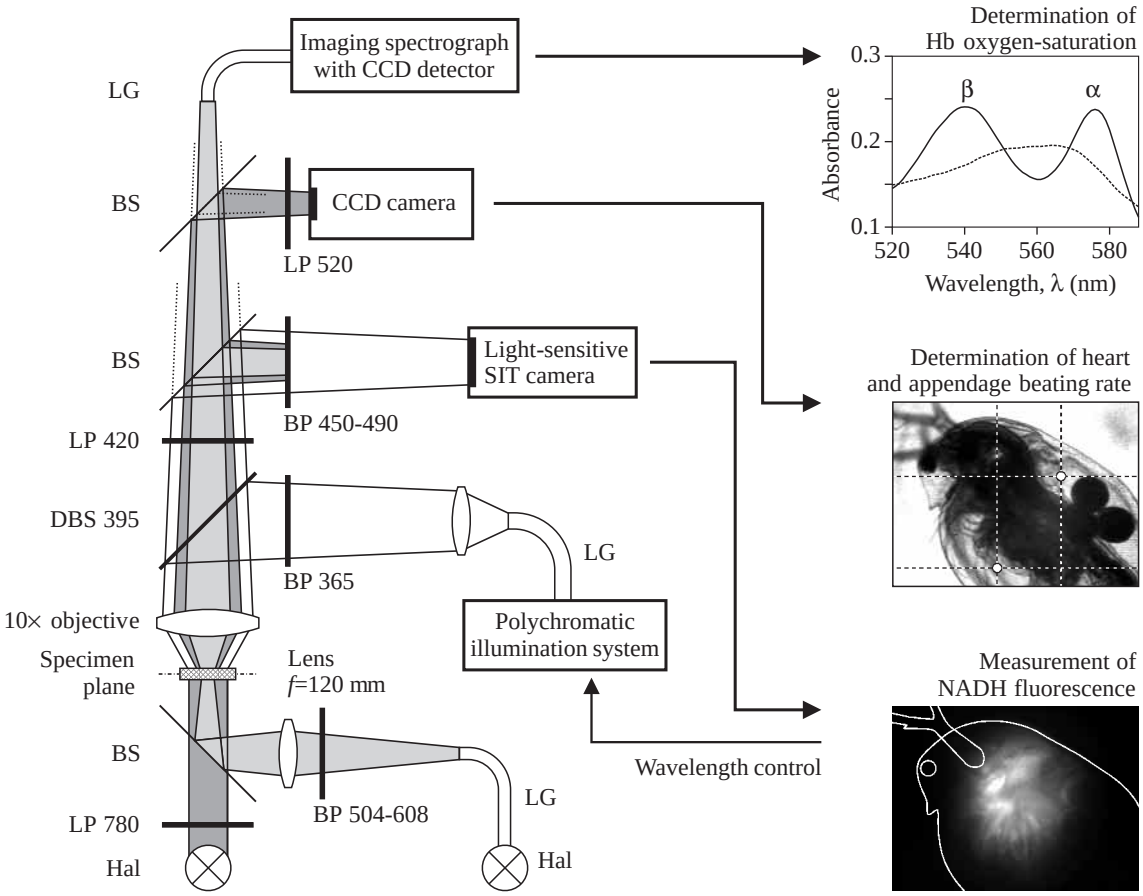

Fig. 1. Microscopic arrangement for the simultaneous measurement of haemoglobin (Hb) oxygen-saturation, heart rate, appendage beating rate and NADH fluorescence. The heart region of the animal was transilluminated with green light in the wavelength range 504–608 nm. Light that passed through this region was analysed spectrally to determine Hb oxygen-saturation. Using infrared transillumination at wavelengths above 780 nm, the periodic movements of the heart and the thoracic appendages were monitored by a light-sensitive CCD camera, and digital motion analysis was used to calculate heart and appendage beating rate. For alignment purposes, a longpass filter (LP 520) in front of the sensitive CCD camera attenuated, but did not completely block, the bright detection light beam used for Hb measurements. The central part of the animal was epi-illuminated with ultraviolet light at 365 nm to excite the pyridine nucleotides in the tissues, and the fluorescence image in the wavelength range 450–490 nm was collected by a light-sensitive SIT camera. The optical paths are visualized by different grey shadings. Dashed lines indicate light reaching the respective detector without having effects on the respective measurement. BP, bandpass filter; BS, beam splitter; DBS, dichroic beam splitter; *f*, focal length; Hal, halogen lamp; LG, light guide; LP, longpass filter; α and β, absorption bands of oxy-Hb.

General description of the microscopic arrangement

The apparatus consisted of an inverted microscope (Zeiss Axiovert 100, Carl Zeiss, Oberkochen, Germany) equipped with three detection systems for measuring Hb oxygen-saturation, heart rate, appendage beating rate and NADH fluorescence (as an indicator of the tissue oxygenation state) (Fig. 1). The selection of appropriate filter sets, separating the spectral windows required for epifluorescence and transmission illumination, permitted the simultaneous, non-interfering optical determination of all variables.

Measurement of haemoglobin oxygen-saturation

Light from a halogen lamp (50 W, Carl Zeiss, Oberkochen, Germany) was spectrally filtered by a combination of two coloured glass filters (VG 14 and OG 515; Schott, Mainz, Germany) to accentuate the spectrum in the wavelength range 504–608 nm (one-tenth-maximum transmission bandwidth) which encloses the α- and β-absorption bands of oxy-Hb and the absorption band of deoxy-Hb (Antonini and Brunori, 1971). This filter combination blocked the spectrum below 500 nm, which otherwise would have influenced the measurement of NADH fluorescence (see below). Guided *via* a quartz fibre-optic light guide (diameter 550 μm), the light was focused onto the specimen plane to a spot size of approximately 250 μm in diameter. This light beam was used to transilluminate the heart region perpendicular to the animal's median plane. The focal illumination ensured that only the haemolymph in the heart and the pericardium was used for the determination of Hb oxygen-saturation. The image of the illumination spot was picked up by a second quartz fibre-optic light guide (diameter 400 μm) which transmitted the light to an imaging spectrograph (SpectraPro-275I; Acton Research

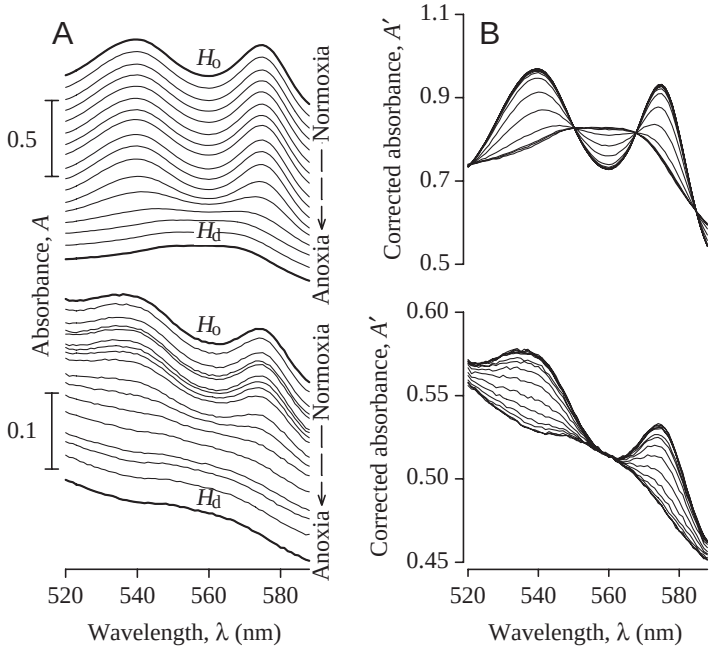

Fig. 2. (A) A sequence of absorption spectra $A(\lambda)$ was obtained from the heart region of haemoglobin (Hb)-rich (above) and Hb-poor (below) animals during a normoxic/anoxic transition experiment. While progressing from the oxygenated to the deoxygenated state, Hb changed its absorbance characteristics, and this can be followed by the disappearance of the maxima at 540 and 576 nm and by the appearance of a broad peak around 560 nm. Note that, because of the difference in Hb concentration, the spectra of the two groups are scaled differently. In addition, the spectra have been displaced vertically by a constant factor to demonstrate better the changes in absorbance. Because of the lower Hb concentration, the spectra of Hb-poor animals appeared to be tilted to the right, which indicates the presence of non-Hb components with higher absorbances in the shorter wavelength range. Moreover, the unequal spacing of spectra reflects fluctuations in the optical properties of the body region analyzed, which were caused by slight body movements of the animal. These effects made it impossible to use reference spectra of purified Hb solutions for the determination of Hb saturation. Instead, *in vivo* spectra, $H_o(\lambda)$ and $H_d(\lambda)$ for oxy-Hb and deoxy-Hb, respectively, obtained under normoxic and anoxic conditions were used for spectral comparisons that permitted the determination of Hb oxygen-saturation and (B) the calculation of corrected absorption spectra $A'(\lambda)$ by applying equations 1 and 2 (see text for details).

Corporation, Acton, MA, USA) equipped with a 16-bit liquid-nitrogen-cooled slow-scan CCD detector (576×384 pixels; LN/CCD-576E, Princeton Instruments, Trenton, NJ, USA). Using a grating with 300 grooves mm^{-1}, intensity spectra were taken in the wavelength range 490–640 nm with a pixel dispersion of 0.261 nm $pixel^{-1}$. An exposure time of 2 s was chosen for spectrum acquisition, which was sufficiently long in comparison with the heart beat cycle that periodic fluctuations in transmittance caused by cardiac contractions did not affect the measurement.

To convert intensity spectra $I(\lambda)$ into absorption spectra $A(\lambda)$, a reference intensity spectrum $I_0(\lambda)$ was taken before the start of the experiment by displacing the experimental chamber slightly so that the animal inside was moved out of the focal detection beam. $A(\lambda)$ was calculated by taking $\log_{10}[I_0(\lambda)]/[I(\lambda)]$, reduced to that part of the spectrum covering the wavelength range 520–588 nm with a wavelength increment of 1 nm, and finally smoothed by a running average using a window of 3 nm. Spectrum acquisition was carried out automatically every 10 s using WinSpec software (Princeton Instruments).

To determine Hb oxygen-saturation, a set of reference spectra $H(\lambda)$ required for spectral comparisons was generated by a weighted summation of oxy-Hb and deoxy-Hb spectra $[H_o(\lambda), H_d(\lambda)]$:

$$H(\lambda) = SH_o(\lambda) + (1-S)H_d(\lambda), \quad (1)$$

where S is the oxygen-saturation coefficient. $H_o(\lambda)$ and $H_d(\lambda)$ were measured separately for each individual and represented essentially the two $A(\lambda)$ collected under normoxic and anoxic conditions, respectively (Fig. 2A). In total, 101 reference spectra $H(\lambda)$ corresponding to 101 different oxygen-saturation levels of Hb was obtained by varying S from 0 to 1.00 in steps of 0.01.

A detailed inspection of the absorption spectra $A(\lambda)$ revealed that a correction to $A(\lambda)$ was required before any spectral comparisons could be performed. This was achieved using the following equation:

$$A'(\lambda) = cA(\lambda) + d, \quad (2)$$

where $A'(\lambda)$ represents the corrected form of $A(\lambda)$ and the regression coefficients c and d account for slight changes in optical pathlength and light scattering, respectively, that resulted from body movements of the animal during enhanced beating activity of the large antennae (Fig. 2). Linear regression analysis was then performed to match $A'(\lambda)$ to each of the 101 reference spectra $H(\lambda)$. Hb oxygen-saturation was derived from the reference spectrum $H(\lambda)$ that yielded the best correspondence with $A'(\lambda)$.

Measurement of heart rate and appendage beating rate

Heart rate and appendage beating rate were measured by digital motion analysis (Paul et al., 1997) using infrared transillumination. As the lateral and the upper photo tube of the microscope were occupied by the two other detection systems, the eyepiece optics had to be removed and replaced with a light-sensitive video camera (HL5-MK; Proxitronic, Bensheim, Germany). The video signal was digitized by a computer equipped with a real-time PCI frame grabber (Meteor/RGB; Matrox, Quebec, Canada). The program computed the frequency of the periodic movements by using the fast Fourier transform algorithm (Press et al., 1992). Heart

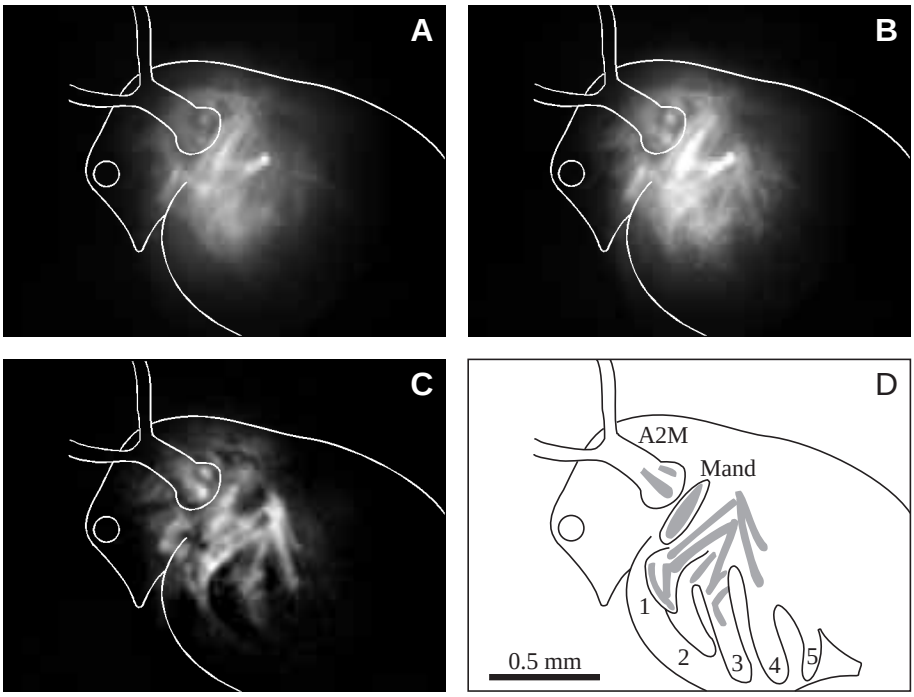

Fig. 3. Localization of NADH fluorescence in *Daphnia magna*. To obtain satisfactory fluorescence images, the excitation light was concentrated on the central portion of the animal. The body region in focus comprised the mandible (Mand), the base of the large antenna (A2M) and the bases of the thoracic limbs (1–5). Switching from normoxia (A) to anoxia (B) resulted in a strong increase in fluorescence intensity, indicating an accumulation of mitochondrial NADH. The difference image (C) reveals that this increase in intensity derived from various groups of muscles associated with the respective appendages (D).

and appendage beating rate were determined every 2 s with a nominal frequency resolution of 2.9 beats min^{-1}. Intermittent or non-periodic movements of the appendages were counted manually by inspecting the video sequences recorded by an S-VHS video recorder (AG-7355, Panasonic).

Measurement of NADH fluorescence

A computer-driven monochromatic illumination system (T.I.L.L. Photonics, Planegg, Germany; 75 W xenon arc lamp, spectral range 260–680 nm, spectral band width 13 nm, response time <2 ms) was used for epifluorescence excitation. The reflector slider of the microscope contained an excitation bandpass filter with a transmittance wavelength of 365 nm, a dichroic beamsplitter with a cut-off wavelength of 395 nm and a long-pass emission filter with a cut-off wavelength of 420 nm (filter set 02; Carl Zeiss). The spectral characteristics of the dichroic mirror and the long-pass emission filter made it possible to analyse Hb oxygen-saturation at the same time. The fluorescence image was scanned by using a light-sensitive silicon-intensified target (SIT) camera (C2400-8, Hamamatsu, Japan; gamma 1.0) attached to the upper camera port of the microscope. An additional bandpass filter (450–490 nm) in front of the SIT camera was needed to prevent optical interference with the Hb measurement.

Because of the weak NADH fluorescence emission, the excitation light was concentrated on the central area of the specimen plane, and the SIT camera operated at maximum sensitivity. To improve the quality of the noisy video images, video sequences of 75 images scaled down to a size of 192×144 pixels were digitally averaged by a computer equipped with a real-time PCI frame grabber (Meteor/RGB). This image-gathering operation was followed by a background subtraction procedure. The excitation wavelength of 365 nm was selected only during fluorescence image acquisition. Otherwise, the wavelength was set to 680 nm and no light reached the specimen, thus avoiding problems such as bleaching effects. Image acquisition was performed every 15 s.

The focus and position of the animal were adjusted in such a way that the muscle groups associated with the mandible and the bases of the limbs contrasted with the blurred background in the faint fluorescence images (Fig. 3). These images were further analysed by calculating mean fluorescence intensities from a rectangular image area comprising these structures.

Selection of animals and experimental conditions

For our experiments, we used females 2.4–2.8 mm long containing 2–4 parthenogenetic embryos of developmental stages 2–3 [see table 3 of (Green, 1956)] in the brood chamber. Egg deposition occurs in *D. magna* approximately 30 min after moulting, whereas stage 2 starts approximately 3 h later and lasts 17 h (at 22 °C; Green, 1956). Stage 2 is characterized by eggs that have markedly granular transparent edges and fat cells that are still in the process of formation. The following stage, lasting approximately 10 h, can be identified by headless embryos with the egg membrane cast off. Since the mother and her brood were in defined stages of the reproductive, moulting and developmental cycles, possible sources of interindividual variation affecting the physiological state of the mother [e.g. heart rate (Meijering, 1958)] or the total rate of oxygen consumption (Glazier, 1991) could be excluded. Before the start of the experiments, the animals were transferred into nutrient-free normoxic medium for 2–12 h. The selection of fasting animals ensured that digestive processes did not affect the rate of oxygen consumption (Lampert, 1986) and systemic functions involved in oxygen transport.

The experiments were carried out at 20 °C in a special

thermostatted perfusion chamber [see (Paul et al., 1997)] that allowed microscopic observation of single animals. Animals were tethered by gluing the apical spine to a resistance wire (0.3 mm in diameter) attached to a plastic cube (4.5 mm side length) with adhesive (histoacryl; B. Braun Melsungen AG, Melsungen, Germany). The block with the tethered animal was placed onto the glass bottom of the perfusion chamber, which was then sealed by screwing the transparent screw top down until the block was contacted. This ensured that the chamber volume and flow velocity within the chamber were constant. The animal was positioned lateral-side-down in the chamber with its head orientated against the flow of medium. The large antennae were free to move, and the animal did not contact the top and bottom of the chamber. The flow rate of the medium was set to 5 ml min^{-1}. The chamber was initially perfused with air-saturated medium, and the animal was allowed to acclimate to these conditions for 30 min. During the experiment, the animal was exposed to a controlled transition from normoxia (20.56 kPa) to anoxia (<0.27 kPa) by gradually decreasing the ambient oxygen partial pressure of the medium according to the profile shown in Fig. 4A (for technical aspects of the modulation of oxygen partial pressure, see Freitag et al., 1998). The profile consisted of 17 steps with a duration of 3 min for each step. This time was sufficient for the animal to attain a new level of Hb oxygen-saturation, heart rate, appendage beating rate and NADH fluorescence intensity (Fig. 4B–E).

Determination of haemolymph Hb concentration

Haemolymph samples were taken from Hb-poor and Hb-rich individuals. The animals were transferred to a microscope slide, and adhering water was gently removed with filter paper. Using very fine spring scissors (no. 15001-08; Fine Science Tools, North Vancouver, Canada), the second antenna was amputated proximally (Fritzsche, 1917) and the oozing haemolymph was aspirated into a 2 µl capillary pipette (minicaps; Hirschmann Laborgeräte, Eberstadt, Germany). Individual haemolymph samples were transferred into a Fuchs–Rosenthal counting chamber (0.02 cm depth), and absorption spectra were measured under oxygenated conditions using water as reference and the arrangement described in Fig. 1. We decided to use water instead of Hb-free haemolymph as a reference since it seemed to be impossible to obtain both whole haemolymph and Hb-free haemolymph from the same individual. This decision, however, made it necessary to consider the spectral contribution of non-Hb components, and this was achieved by some additional computations elaborated in the Results section. The Hb concentration was determined according to Lambert–Beer's law.

Data processing and statistical analyses

To relate Hb oxygen-saturation, heart rate, appendage beating rate and fluorescence intensity to ambient oxygen partial pressure, their temporal profiles (Fig. 4B–D) were analysed to calculate mean values for each variable for the last minute of each step change in oxygen partial pressure. Data are expressed, unless stated otherwise, as mean values ± standard deviation (S.D.), with *N* indicating the number of

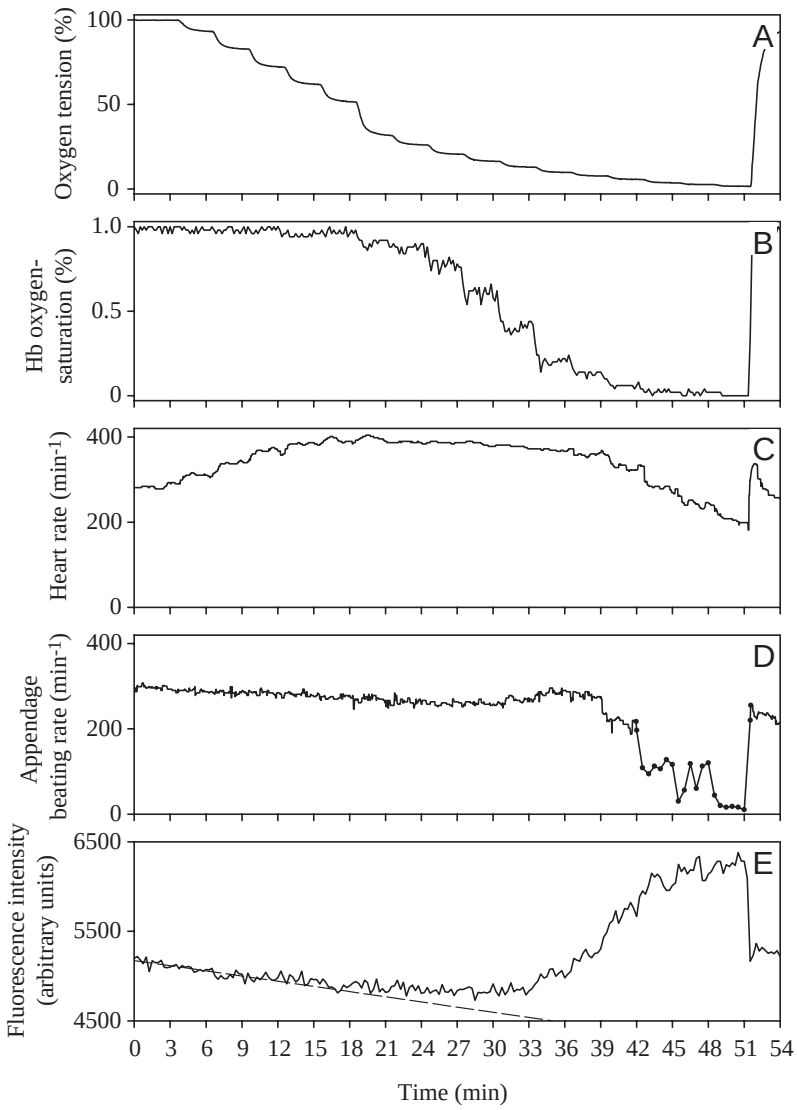

Fig. 4. Temporal organization of the experiment. The animal was exposed to a controlled, gradual transition from normoxia to anoxia (A) while haemoglobin (Hb) oxygen-saturation (B), heart rate (C), appendage beating rate (D) and NADH fluorescence intensity (E) were measured continuously. At very low oxygen tensions, the thoracic appendages showed an irregular rather than a periodic temporal pattern of movement. Therefore, appendage beating rate was counted manually every 30 s (as indicated by the filled circles). NADH fluorescence always showed a linear decline in intensity which, at a certain low level of oxygen tension, was superimposed by the hypoxia-induced increase in mitochondrial NADH content. The data were therefore trend-corrected by calculating a linear regression line (dashed line) for the initial 12–18 min of the experiment during which Hb oxygen-saturation remained unchanged.

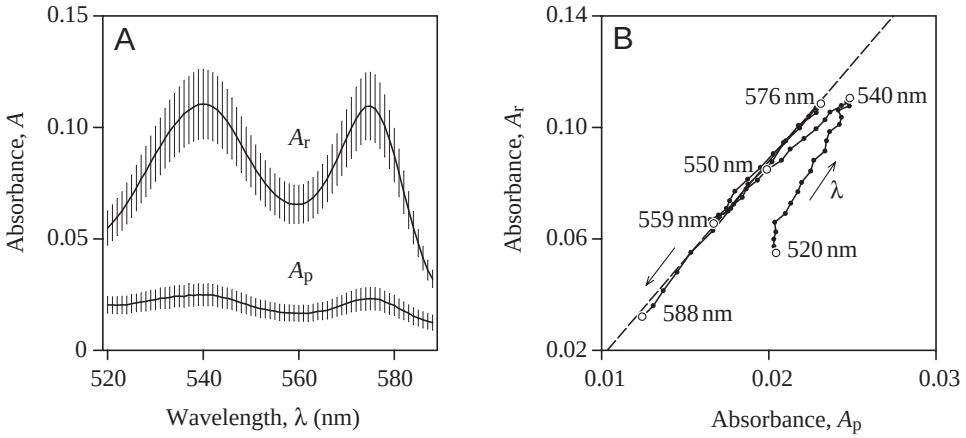

Fig. 5. (A) Absorption spectra $A_r(\lambda)$ and $A_p(\lambda)$ of haemolymph samples obtained from haemoglobin (Hb)-rich and Hb-poor animals (N=5 each), respectively, were measured under oxygenated conditions in a counting chamber with an optical pathlength of 0.02 cm using water as a reference. The absorption maxima at 540 nm and 576 nm indicate the presence of Hb in both haemolymph samples. Data are given as means ± S.E.M. (B) Plotting $A_r(\lambda)$ against $A_p(\lambda)$ showed that data pairs within the wavelength range 550–588 nm fall on a straight line ($A_r=k_1A_p+k_0$, with k_0=–0.0526 and k_1=7.015, r^2=0.993, N=39). Data pairs in the lower wavelength range deviated from this line, indicating that components other than haemoglobin contributed to the absorbance of the haemolymph sample in a wavelength-dependent manner.

animals examined. Sigmoidal curves were generated by nonlinear regression analysis using the Hill equation. Mean regression lines were obtained by averaging the variables of individual regression lines. Statistical differences in mean values were assessed using the *t*-test after differences in variance had been checked using the *F*-test. When variances differed, the unequal-variance *t*-test was applied to assess the difference between means. Statistical differences were considered significant at P<0.05.

Results

Haemolymph Hb concentrations

Absorption spectra were measured from haemolymph samples obtained from single Hb-rich and Hb-poor individuals (Fig. 5A). The choice of water instead of Hb-free haemolymph as a reference made it possible that components other than haemoglobin could contribute to the absorption spectrum. Particularly at low Hb concentrations, this could offset the contribution to the spectrum of Hb. Neglecting this effect would lead to an overestimation of Hb concentration when applying Lambert–Beer's law. The following two equations were therefore used to account for the spectral contribution of non-Hb components:

$$A_r(\lambda) = C_r H_o(\lambda) + b\,, \tag{3}$$

$$A_p(\lambda) = C_p H_o(\lambda) + b\,, \tag{4}$$

where $A_r(\lambda)$ and $A_p(\lambda)$ are the haemolymph absorption spectra of Hb-rich and Hb-poor animals, respectively, $H_o(\lambda)$ is the absorption spectrum of oxygenated Hb, and C_r and C_p are the respective relative measures of Hb concentration. The variable b, reflecting the contribution of non-Hb components to the absorption spectra, was assumed to be wavelength-independent and to have the same value for Hb-rich and Hb-poor animals. Provided that there are no differences in the absorbance characteristics of Hb in the two groups, equations 3 and 4 can be combined into the following equation:

$$A_r(\lambda) = k_1 A_p(\lambda) + k_0\,, \tag{5}$$

where

$$k_1 = \frac{C_r}{C_p} \tag{6}$$

and

$$k_0 = b(1 - k_1)\,. \tag{7}$$

Plotting $A_r(\lambda)$ against $A_p(\lambda)$ revealed a linear relationship for the wavelength range 550–588 nm (Fig. 5B), which is to be expected if the two spectra are identical except for differences arising from additive and multiplicative factors (see equation 5). Data pairs belonging to the lower wavelength range 549–520 nm, however, deviated from this straight line, indicating that non-Hb components made a wavelength-dependent contribution to the absorption spectra. Linear regression analysis was therefore performed in the wavelength range 550–588 nm, for which the assumption of a wavelength-independent value of b holds, yielding values of –0.0526 for k_0 and 7.015 for k_1 (r^2=0.993, N=39 data points). As k_1 reflects the ratio of Hb concentration between Hb-rich and Hb-poor animals, it becomes obvious that the Hb concentration of Hb-rich animals was seven times that of Hb-poor animals.

The contribution of non-Hb components to the absorption spectrum (b) was 0.0087. Subtracting this value from the absorbances at 576 nm (Hb-rich, 0.1085±0.0152; Hb-poor, 0.0231±0.0051; mean ± S.E.M., N=5 each) permitted the calculation of absolute Hb concentrations by applying Lambert–Beer's law. Using the millimolar extinction coefficient ε_{576} of 14.8 mmol l^{-1} cm^{-1} for *D. magna* Hb (Hoshi and Kobayashi, 1971) and an optical pathlength of 0.02 cm (counting chamber), the haem-based Hb concentrations of Hb-rich and Hb-poor *D. magna* were 337.2±51.4 μmol l^{-1} and 48.6±17.2 μmol l^{-1}, respectively.

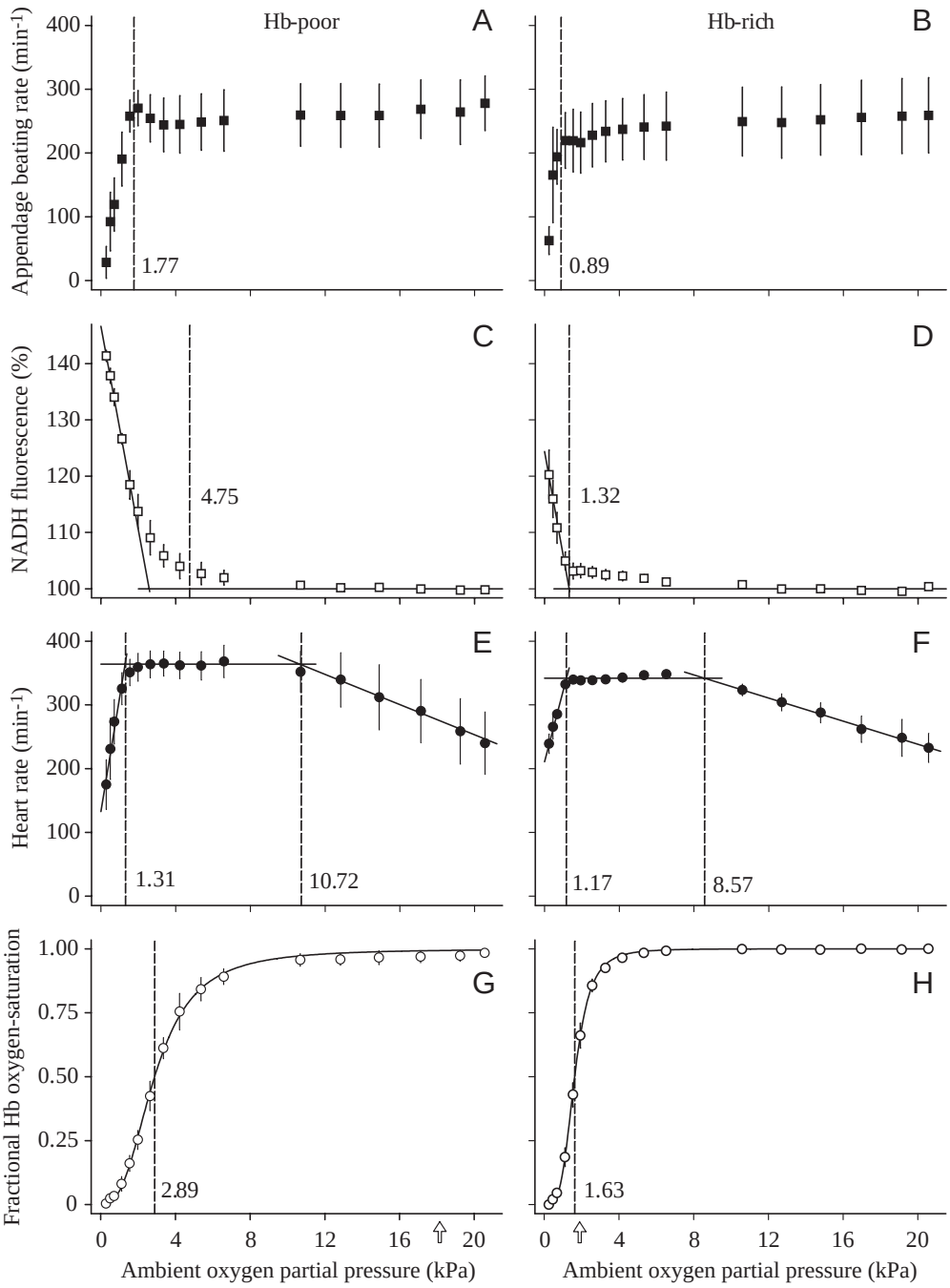

Fig. 6. Responses of appendage beating rate, NADH fluorescence intensity, heart rate and haemoglobin (Hb) oxygen-saturation of normoxia-acclimated Hb-poor (left) and hypoxia-acclimated Hb-rich *Daphnia magna* (right) to decreasing ambient oxygen partial pressures (P_{O_2amb}). Each data point represents the mean ± S.D. (N=6). Solid lines represent either plateaus in the physiological data or mean regression lines obtained by averaging the variables of individual regression lines. Dashed lines and the respective values represent critical P_{O_2amb} values, marking the significant decrease in appendage beating rate, the intersection of two solid lines or the P_{O_2amb} at which 50 % of the Hb was saturated. The only exception concerns the critical P_{O_2amb} in C (see Fig. 7). NADH fluorescence intensity was trend-corrected (see Fig. 4E) and normalized to 100 %. Sigmoidal curves were generated by nonlinear regression analysis using the Hill equation, which yielded the P_{O_2amb} at which 50 % of Hb was saturated, and the Hill coefficient n as a measure of sigmoidity (r^2>0.990 for both curves). The two arrows on the abscissa indicate the P_{O_2amb} at which the animals were reared.

Systemic responses to hypoxia

The tolerance of oxygen deficiency was tested in Hb-rich and Hb-poor *Daphnia magna* by gradually lowering the oxygen partial pressure of the ambient medium (P_{O_2amb}) while (i) appendage beating rate, (ii) NADH fluorescence intensity, (iii) heart rate and (iv) Hb oxygen-saturation were measured simultaneously (Fig. 6A–H).

The appendage beating rate f_A of Hb-poor and Hb-rich animals decreased slightly (1.59 *versus* 1.28 $min^{-1}\,kPa^{-1}$) when P_{O_2amb} was lowered from 20.5 to 4.0 kPa (Fig. 6A,B). Within this range, the mean f_A of Hb-poor animals was always higher, on average by 10 beats min^{-1}, than that of Hb-rich animals. The two f_A profiles appeared to be aligned parallel to each other until the reduction in P_{O_2amb} below 2.95 kPa induced diverging changes in f_A (Fig. 7). In Hb-poor animals, mean f_A started to increase and reached a maximum at 2 kPa before it dropped significantly below 1.77 kPa (Fig. 6A). The elevation in f_A around 2 kPa occurred in all six individuals. In Hb-rich animals, mean f_A decreased slightly at first but then appeared to plateau until P_{O_2amb} dropped below 0.89 kPa (Fig. 6B). This intermediate plateau, however, did not reflect a uniform response of the Hb-rich animals but concealed a greater variability in individual f_A. When P_{O_2amb} approached anoxic values (<0.27 kPa), the f_A of Hb-poor animals was

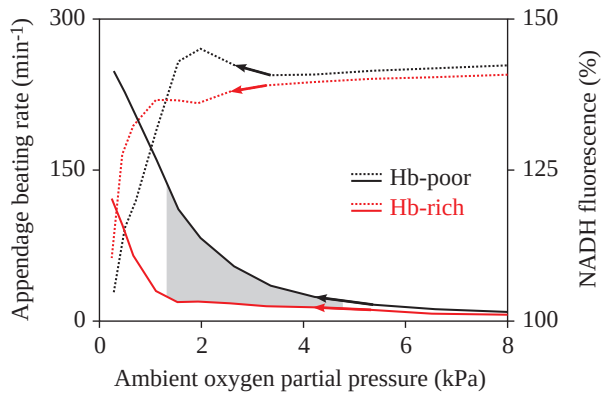

Fig. 7. Detailed representation of the data of Fig. 6A–D. The appendage beating rate (f_A) profiles (dotted lines) of haemoglobin (Hb)-poor and Hb-rich animals appeared to be aligned parallel to each other until the reduction in ambient oxygen partial pressure (P_{O_2amb}) from 3.3 to 2.6 kPa (mean 2.95 kPa) induced significantly diverging changes in f_A (Hb-poor, Δf_A=+10.23±12.70 min^{-1}; Hb-rich, Δf_A=–6.19±5.06 min^{-1}; unpaired two-tailed *t*-test: t=2.94, d.f.=10, P=0.01; means ± S.D., N=6). Similar diverging changes were initiated in NADH fluorescence intensity I_{NADH} (solid lines) when the P_{O_2amb} was reduced from 5.3 to 4.2 kPa (mean 4.75 kPa) (Hb-poor ΔI_{NADH}=+1.30±0.80 min^{-1} *versus* Hb-rich ΔI_{NADH}=+0.42±0.44 min^{-1}; unpaired two-tailed *t*-test: t=2.36, d.f.=10, P=0.04; means ± S.D., N=6). This divergence in I_{NADH} extended over the P_{O_2amb} range from 4.75 to 1.32 kPa (shaded area), where I_{NADH} of Hb-rich animals appeared to stabilize at 103 %, whereas that of Hb-poor animals rose from 104 to 123 %. Note that, in Hb-poor animals, the increase in f_A at 2 kPa coincided with the increase in I_{NADH}. Arrows indicate significantly diverging responses in the respective variables. The standard deviations of the curves have been omitted for clarity.

significantly lower than that of Hb-rich animals (Hb-poor 28.60±24.95 min^{-1}, N=5; Hb-rich 63.33±19.62 min^{-1}, N=6; unpaired two-tailed *t*-test: t=–2.59, d.f.=9, P=0.03).

The fluorescence emitted from the proximate parts of the appendage muscles always showed a linear decline in intensity which, at a certain low level of P_{O_2amb}, was superimposed by the hypoxia-induced increase in NADH (Fig. 4E). To consider only these hypoxia-induced changes in fluorescence intensity, a trend correction was applied to the data (Fig. 4E).

During normoxia and moderate hypoxia (20–5 kPa), there was no change in the trend-corrected NADH fluorescence intensity (I_{NADH}) in either group (Fig. 6C,D). A reduction in P_{O_2amb} below 4.75 kPa induced significantly divergent responses in I_{NADH} of Hb-poor and Hb-rich animals (Fig. 7). The I_{NADH} of Hb-poor animals rose with increasing negative slope before finally attaining a constant slope of –18.03±1.85 % kPa^{-1} (N=6) (Fig. 6C). This final linear increase in I_{NADH} also occurred in Hb-rich animals (Fig. 6D), and the slopes (–18.45±3.02 % kPa^{-1} for Hb-rich animals, N=6) were not statistically different (unpaired two-tailed *t*-test: t=0.29, d.f.=10, P=0.78), indicating a similar strength of response in ΔI_{NADH} to progressive severe hypoxia. However, before entering the final steep part of the profile, I_{NADH} of Hb-rich animals appeared to settle to a constant level rather than rising overproportionately as it did in the Hb-poor animals (Fig. 7). The final steep increase did not occur until P_{O_2amb} had reached the critical level of 1.32 kPa, a value obtained by calculating the intersection of the regression line and the 100 % intensity level (Fig. 6D). As a consequence of this 'delayed' response, Hb-rich animals attained a significantly lower maximum level of I_{NADH} than Hb-poor animals (120.33±3.91 % *versus* 141.38±0.99 %, N=6 each; unpaired two-tailed *t*-test: t=12.79, d.f.=5.65, P<0.01). In summary, within the P_{O_2amb} range 4.75–1.32 kPa, a stabilization of I_{NADH} seemed to occur in Hb-rich animals, whereas the I_{NADH} of Hb-poor animals rose steadily.

The response of heart rate f_H followed a three-phase pattern (Fig. 6E,F), initiated by a linear increase when the P_{O_2amb} started to decline, followed by a plateau, and then by a steep decrease when P_{O_2amb} approached anoxic values. Hb-poor animals showed a stronger increase in f_H that was reflected by the steeper slope $f_H/\Delta P_{O_2amb}$ (Hb-poor, –11.82±1.84 min^{-1} kPa^{-1}; Hb-rich, –9.05±2.20 min^{-1} kPa^{-1}, N=6 each; unpaired two-tailed *t*-test: t=–2.36, d.f.=10, P=0.04). They attained a somewhat higher plateau in f_H (363.79±21.62 min^{-1}) which, however, was not statistically different from that of Hb-rich animals (341.72±5.74 min^{-1}; unpaired two-tailed *t*-test: t=2.42, d.f.=5.70, P=0.05). Hb-poor animals entered this plateau at a higher P_{O_2amb} than Hb-rich animals (10.72±2.04 kPa *versus* 8.57±1.07 kPa; unpaired two-tailed *t*-test: t=2.29, d.f.=10, P=0.04). However, the P_{O_2amb} that caused the abrupt decline in f_H was not statistically higher in Hb-poor (1.31±0.21 kPa) than in Hb-rich animals (1.17±0.06 kPa; unpaired two-tailed *t*-test: t=1.60, d.f.=5.73, P=0.16). During anoxia (<0.27 kPa), f_H of Hb-poor animals was significantly lower than that of Hb-rich animals (174.90±38.98 min^{-1} *versus* 237.87±13.90 min^{-1}; unpaired two-tailed *t*-test: t=–3.73, d.f.=6.25, P<0.01).

In both groups, Hb was fully saturated in the heart region during incipient hypoxia but, with further reduction in P_{O_2amb}, it decreased earlier in Hb-poor than in Hb-rich animals (Fig. 6G,H). The relationships between Hb oxygen-saturation and P_{O_2amb} could be conveniently described by sigmoid Hill curves (r^2>0.990 for all individual regression lines). The half-oxygen-saturation P_{50} was significantly higher in Hb-poor than in Hb-rich animals (2.89±0.15 kPa *versus* 1.63±0.10 kPa, N=6 each; unpaired two-tailed *t*-test: t=17.45, d.f.=10, P<0.01). In addition, the Hill coefficient n, as a measure of sigmoidity, was also significantly different (Hb-poor, 2.73±0.45 kPa; Hb-rich, 3.90±0.37 kPa, N=6 each; unpaired two-tailed *t*-test: t=–4.89, d.f.=10, P<0.01), indicating that the *in vivo* saturation curves of Hb-poor and Hb-rich animals deviated from each other in position and shape.

Discussion

The Cladocera have evolved a variety of strategies and adaptations to cope with the selective pressures exerted by a variable aquatic environment (Fryer, 1991; Fryer, 1996). In those species that rise to the challenge of environmental

Table 1. *Properties of the haemoglobin of* Daphnia magna *at 20 °C*

P_{50} (kPa)	*n*	Description of the animals	Hb concentration	Reference
Purified Hb solutions[a]				
0.51–0.71	1.2–1.3	Pale	20–30 mg g^{-1} dry mass	3
0.47		Pink	0.15–0.20 mg g^{-1} wet mass	1
0.23	1.6	Hb-rich	8–12 g l^{-1} haemolymph	4
0.15–0.21	1.5–1.6	Red	75–120 mg g^{-1} dry mass	3
In vivo				
4.67[b]		Hb-poor	25 mg g^{-1} dry mass	5
2.89		Hb-poor	49 μmol l^{-1} haemolymph	6
2.67[b]		Pink		2
2.00[b]		Hb-rich	84 mg g^{-1} dry mass	5
1.63		Hb-rich	337 μmol l^{-1} haemolymph	6

Hb, haemoglobin.

[1]Sugano and Hoshi, 1971; [2]Hoshi and Yahagi, 1975; [3]Kobayashi et al., 1988; [4]Kobayashi et al., 1990a; [5]Kobayashi and Tanaka, 1991; [6]the present study.

[a]0.1 mol l^{-1} phosphate buffer (pH 7.4) and, when explicitly stated in the respective paper, at 0 % CO_2.

[b]Animals 2.8 mm long.

oxygen deficiency, the increase in Hb concentration reflects such an adaptive process. This change has immediate consequences for physiological performance and can have far-reaching effects on the ecological fitness of the organism. The present study was carried out to determine the physiological role of Hb and to obtain a more profound understanding of the importance of Hb in the Cladocera.

Differences in Hb concentration

Hypoxic pre-incubation (8–10 % air saturation, 21.0–23.0 °C) of juvenile *Daphnia magna* over a period of 10 days resulted in a sevenfold elevation of Hb concentration in the haemolymph, which lay within the range of increase described for *D. magna* and other related species (Fox et al., 1951; Chandler, 1954; Kobayashi, 1982; Kobayashi and Hoshi, 1982; Carvalho, 1984; Kobayashi and Nezu, 1986). A comparison of absolute values instead of relative differences is not always possible, because many data are given as dry-mass-specific Hb concentrations (Table 1) or as relative measures (Hb index method) (Fox, 1948; Green, 1956; Carvalho, 1984). Kobayashi and Hoshi (Kobayashi and Hoshi, 1982) reported Hb concentrations varying from 1 g l^{-1} for Hb-poor *D. magna* kept under normoxic/hyperoxic conditions to 16 g l^{-1} for Hb-rich animals kept at approximately 8 % air saturation. Using the calculated molecular mass of 36 kDa for a two-domain subunit (Tokishita et al., 1997; Kimura et al., 1999), these figures translate into haem-based concentrations of 55 and 888 μmol l^{-1}, respectively. The lower value corresponds well with the 49 μmol l^{-1} of our Hb-poor, normoxic animals. The Hb concentration of our Hb-rich, hypoxic animals was 337 μmol l^{-1}, which represents 40 % of the maximum value found by Kobayashi and Hoshi (Kobayashi and Hoshi, 1982). Responses to almost the same level of hypoxia could be affected by various factors including temperature, the duration of hypoxic incubation (Kring and O'Brien, 1976; Carvalho, 1984; Kobayashi et al., 1990b), food availability, moulting, reproduction and maternal influences (Dresel, 1948; Fox et al., 1949; Green, 1956; Kobayashi et al., 1990a). In addition, Weider and Lampert (Weider and Lampert, 1985) have shown that *Daphnia* clones can differ considerably in their ability to synthesize Hb.

Selection of animals and the experimental regimen

Some general remarks are necessary to address the comparability of data on the hypoxia-tolerance of *D. magna* before an interpretation of our experimental results is given in the following sections. Several laboratory studies have shown that filtering and respiration rates of Hb-poor *D. magna* and the closely related *D. pulex* have already started to decline at critical oxygen concentrations of 1.3–3.0 mg O_2 l^{-1} (Kring and O'Brien, 1976; Heisey and Porter, 1977; Kobayashi and Hoshi, 1984). In our Hb-poor *D. magna*, we found that appendage beating rate did not decrease until P_{O_2amb} had reached 1.77 kPa, which corresponded to 0.77 mg O_2 l^{-1}.

It appears that our Hb-poor animals exhibited a higher tolerance for environmental oxygen deficiency which, however, can be attributed to the stringent selection of experimental animals and the specific experimental regimen that was designed to reveal Hb-derived effects. First, animals entering the experiment were in a defined low metabolic state, fasting, and with not more than four early embryos in the brood chamber [see (Lampert, 1986; Bohrer and Lampert, 1988; Glazier, 1991)]. Second, these animals were within the first half of their moulting cycle and, thus, the formation of the new cuticle under the old one had not progressed far enough to become relevant as an additional diffusive barrier for oxygen. Third, animals were positioned in the experimental chamber in the middle of the water column and were continuously perfused with fresh medium, thus preventing localized oxygen depletion around the animal. Fourth, the experimental

temperature in the studies of Kring and O'Brien (Kring and O'Brien, 1976) and Heisey and Porter (Heisey and Porter, 1977) was 2–4 °C higher than in our experiments. An increase in temperature is known to shift the critical oxygen concentration towards higher values (Herreid, 1980). Finally, the exposure to 'critical' oxygen levels (<3 mg O_2 l^{-1}) lasted no longer than 30 min. It seems likely that, for energetic reasons, our Hb-poor animals would not be able to sustain their high appendage beating rates under chronic exposure to 0.77 mg O_2 l^{-1}. The NADH fluorescence signal of the limb muscles indicated a limitation to oxygen supply and an activation of anaerobic energy provision at 2.07 mg O_2 l^{-1} (4.75 kPa; see below).

The meaning of the NADH fluorescence signal

The measurement of NADH fluorescence has become the optical method of choice for assessing cellular redox state in tissue (Chance, 1991). Irrespective of the relative contributions of mitochondrial and cytoplasmatic NAD(P)H to total fluorescence intensity, it is the increase in signal intensity during an aerobic/anaerobic transition that can primarily be related to the accumulation of mitochondrial NADH (Wakita et al., 1995; Paul et al., 2000). We therefore used this variable as an indicator for oxygen deficiency in the limb muscle tissue of *Daphnia magna*.

Below an ambient oxygen partial pressure (P_{O_2amb}) of 4.75 kPa, the NADH fluorescence intensity (I_{NADH}) of Hb-poor animals started to rise in a manner that clearly deviated from that in Hb-rich animals. In the latter, I_{NADH} appeared to be stabilized within the range 4.75–1.32 kPa, and it did not rise until P_{O_2amb} fell below 1.32 kPa. Taking into account the fact that Hb concentration was seven times higher in Hb-rich animals than in Hb-poor animals, it is very likely that the extra Hb was responsible for the stabilization of I_{NADH}. Hb can achieve such a stabilizing effect because of its nonlinear oxygen-binding characteristics that make it possible to reduce the drop in oxygen partial pressure (P_{O_2}) needed to liberate a given proportion of total oxygen (Jones, 1972). This P_{O_2} buffering occurs when Hb is progressively unloaded along the steepest and physiologically relevant part of its oxygen equilibrium curve. Since information on oxygen equilibrium curves is available for purified solutions of *D. magna* Hb (Table 1), it is, in principle, possible to predict the P_{O_2} in the vicinity of the limb muscle tissue for that P_{O_2amb} range within which our Hb-rich animals had a physiological advantage over Hb-poor animals. For example, from the data obtained from Hb-rich (red) animals (Table 1) (Kobayashi et al., 1988; Kobayashi et al., 1990a), it can be calculated that approximately 80 % of bound oxygen is released from Hb when the P_{O_2} declines from 0.90 to 0.05 kPa, a range that includes the steepest part of the oxygen equilibrium curve. Provided that these *in vitro* oxygen-binding characteristics also hold *in vivo* in the haemolymph of Hb-rich *D. magna*, it is conceivable that P_{O_2} in the vicinity of the limb muscle tissue declined within the range 0.90–0.05 kPa when the P_{O_2amb} was reduced from 4.75 to 1.32 kPa.

A comparison of our tissue-specific data on I_{NADH} with those for whole-animal responses [body lactate content, the rate of oxygen consumption (Usuki and Yamagushi, 1979; Kobayashi and Hoshi, 1984)] revealed interesting correspondences. In both Hb-poor and Hb-rich animals, the increase in I_{NADH} coincides with a drop in oxygen consumption and a rise in body lactate levels (Fig. 8). Lactate is probably the main end-product of anaerobic metabolic pathways in *D. magna* (Paul et al., 1998). The close correlation between these variables strongly suggests that the increase in I_{NADH} signalled not only the incipient impairment of the oxygen supply to the limb muscles but also the activation of anaerobic energy provision. The fact that the I_{NADH} of both groups had started to increase while limb beating activity still remained at a high level indicates that a proportion of the energy required was provided by mechanisms of anaerobic energy transformation.

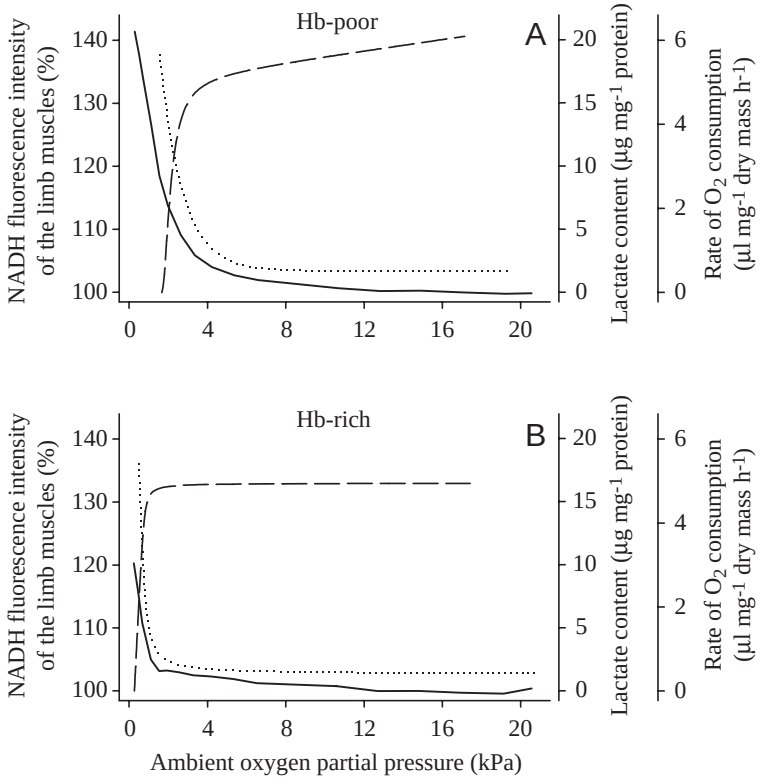

Fig. 8. Comparison of tissue-specific (solid line, NADH fluorescence intensity of the limb muscles; this study) and whole-animal (dotted line, lactate content; dashed line, rate of oxygen consumption) responses of haemoglobin (Hb)-poor (A) and Hb-rich *Daphnia magna* (B) to different ambient oxygen partial pressures (P_{O_2amb}). Lactate determination was performed using animals 1.7–2.0 mm long incubated at different values of P_{O_2amb} for 1 h at 22 °C (Usuki and Yamagushi, 1979). The rate of oxygen consumption (dashed line) was measured in animals 2.5 mm long at 20 °C using a closed respirometry system (Kobayashi and Hoshi, 1984).

Interpretation of in vivo *saturation curves*

Hb oxygen-saturation was measured in the circulatory system of *Daphnia magna* while exposing the animal to a progressive reduction in P_{O_2amb}. To describe the relationship between *in vivo* Hb oxygen-saturation and P_{O_2amb}, we propose using the term *in vivo* 'saturation curve' to avoid confusion with the 'oxygen equilibrium curve'. The latter term is employed in physiology to describe the functional relationship between Hb oxygen-saturation and the oxygen partial pressure in the immediate environment of the Hb molecule, e.g. (Randall et al., 1997).

Relating *in vivo* Hb oxygen-saturation to P_{O_2amb}, which essentially represents the oxygen partial pressure in the remote environment of the Hb molecule, has important consequences for the interpretation of the data. In contrast to the oxygen equilibrium curve, which reflects the intrinsic oxygen-binding properties of Hb, the *in vivo* saturation curve is additionally affected by the measurement position, by the Hb concentration, by the rate of oxygen consumption and by the performance characteristics of the circulatory and ventilatory systems (Fig. 9). The *in vivo* saturation curve of a defined haemolymph region can therefore be considered as a functional response curve that integrates the molecular properties of Hb with the systemic characteristics of the organism.

In the present study, the *in vivo* saturation curve was measured in the heart region which, with respect to the model shown in Fig. 9A, can be regarded as a proximate position downstream of the respiratory gas exchanger. At this position, freshly oxygenated haemolymph from the carapace lacuna becomes mixed with less well-oxygenated haemolymph from the dorsal lacuna of the trunk (Pirow et al., 1999b) before it is pumped into the body to provide oxygen to the tissues. This makes the heart region a suitable location to estimate, for example, the total amount of oxygen transported into the body.

The *in vivo* saturation curves of Hb-poor and Hb-rich animals showed that Hb remained almost fully saturated at progressive moderate hypoxia (P_{O_2amb}>10 kPa) but that saturation started to decline with a further reduction in P_{O_2amb}. Half-oxygen-saturation was reached at 2.89 kPa in Hb-poor animals and at 1.63 kPa in Hb-rich animals, respectively. These values are approximately 20–40 % lower than those given by Kobayashi and Tanaka (Kobayashi and Tanaka, 1991; Table 1), and we attribute this to differences in the experimental conditions (e.g. flow rate) and in the characteristics of the animals (body size, the rate of oxygen consumption).

A comparison of the *in vivo* saturation curve with the corresponding oxygen equilibrium curve reveals interesting information concerning the difference in oxygen partial pressure that existed between the ambient medium and the heart region of the animal. This can conveniently be achieved for the half-saturation level by calculating the difference between the corresponding oxygen partial pressures. For example, purified Hb solutions obtained from Hb-poor *D. magna* showed half-saturation at approximately 0.61 kPa (Kobayashi et al., 1988; Table 1). Subtracting this value from 2.89 kPa, which was the P_{O_2amb} at which Hb in the heart region was 50 % saturated, yields a difference of 2.28 kPa. For Hb-rich animals (Table 1), this calculation yields a difference of 1.44 kPa. It is possible that these two values slightly overestimate the real differences because whole-blood samples of *D. magna* seem to have a somewhat lower oxygen-affinity than purified Hb solutions (B. Becher, personal communication). Nevertheless, the fact that this value for Hb-rich animals was approximately 40 % lower than that for Hb-poor animals clearly illustrates that hypoxic acclimation enables *D. magna* to mitigate the decrease in oxygen partial pressure between the ambient medium and the haemolymph in the cardiac region.

Physiological consequences of haemoglobin in Daphnia magna

In *Daphnia*, the persistent and steady movement of the thoracic appendages plays an important role in both food

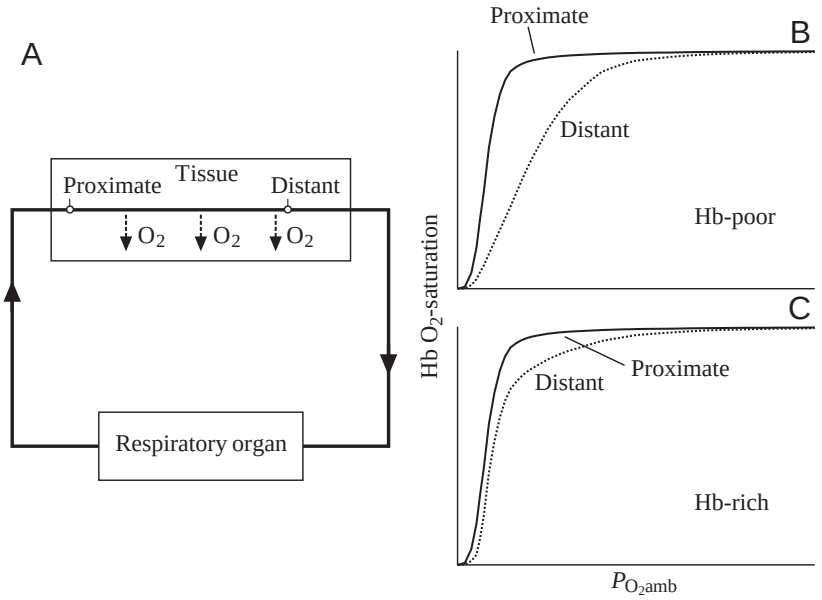

Fig. 9. The *in vivo* saturation curve describes the relationship between haemoglobin (Hb) oxygen-saturation, measured in the circulatory system of an animal, and the oxygen partial pressure of the ambient medium (P_{O_2amb}). The shape and position of the *in vivo* saturation curve are highly variable because they depend not only on the intrinsic oxygen-binding properties of Hb but also on the respective position in the circulatory system, on the haemolymph concentration of Hb and on the systemic and metabolic characteristics of the animal. A simple model of the circulatory system (A) demonstrates the positional effect and the influence of Hb concentration. Oxygenated haemolymph leaves the respiratory organ and enters the tissue compartment where, at the proximate position, the *in vivo* saturation curve is measured (solid lines in B and C). Because oxygen is released from Hb and transferred to the metabolizing tissue, the *in vivo* saturation curve measured at the distant position appears to be shifted to the right (dotted lines). This rightward shift is more pronounced at lower (B) than at higher (C) Hb concentrations.

acquisition and gas exchange (Fryer, 1991; Pirow et al., 1999a). The vital importance of this activity renders this behaviour suitable for analysing the effects of Hb on the physiological performance of the organism. As expected from studies focusing on filtering and respiration rates (Kring and O'Brien, 1976; Kobayashi and Hoshi, 1984), Hb-poor and Hb-rich *D. magna* clearly differed in their ability to sustain the high pumping activity of the thoracic limbs when exposed to a progressive reduction in P_{O_2amb}. Initially, at moderate hypoxia, the appendage beating rate (f_A) of both groups decreased slightly, but still remained at a high level. Reducing P_{O_2amb} below 2.95 kPa induced diverging changes in f_A, a transient increase in Hb-poor animals, which can be interpreted as hyperventilation, and a slight decline to a somewhat lower plateau in Hb-rich animals. The high level of f_A for both groups was abruptly reduced when approaching severe hypoxia, at which point f_A decreased rapidly. In Hb-poor animals, limb movements began to be impeded at 1.77 kPa, whereas Hb-rich animals were able to sustain their limb beating activity until P_{O_2amb} reached a critical level of 0.89 kPa.

A profound mechanistic explanation for these differences can only be achieved when taking into account the impact of Hb on the oxygen-transport characteristics of the circulatory system, as it is in this compartment that Hb exerts its function. This required not only knowledge of Hb concentration and the *in vivo* saturation curve but also information on perfusion rate. Heart rate has proved to be an adequate relative measure that reflects any changes in perfusion rate because stroke volume, which in addition to heart rate determines perfusion rate, was found not to vary greatly when *D. magna* were exposed to hypoxic conditions (Paul et al., 1997; for anoxia-induced variations in stroke volume, see Paul et al., 1998).

Marked changes in heart rate occurred at moderate (>9 kPa) and severe (<1.3 kPa) hypoxia. Reducing P_{O_2amb} from 20 to 9 kPa caused a progressive tachycardia that was slightly less pronounced in Hb-rich than in Hb-poor animals, causing a 6 % higher maximum heart rate in Hb-poor animals. This result, although not statistically significant, could be interpreted as compensation for a lower concentration of Hb and, consequently, for a lower oxygen-carrying capacity of the haemolymph. Alternatively, Hb-rich animals could be prevented from attaining the same maximum heart rate because their higher Hb concentration increased haemolymph viscosity and, thereby, the mechanical load on the heart. The fact that tachycardia developed in both groups within almost the same range of P_{O_2amb} was an unexpected result because a sevenfold higher Hb concentration should allow Hb-rich animals to activate circulatory compensations at a far lower value of P_{O_2amb}. Nevertheless, it is interesting to note that, in both groups, the I_{NADH} of the limb muscles did not increase as long as a reduction in P_{O_2amb} was countered by an increase in heart rate. This observation strongly points to the functional importance of tachycardia in maintaining oxygen delivery to the tissues by increasing tissue perfusion.

The heart rate of both groups settled at a plateau level when P_{O_2amb} dropped below 9 kPa. This plateau was broken below the critical P_{O_2amb} of 1.31 kPa (Hb-poor) and 1.17 kPa (Hb-rich), and heart rate decreased rapidly, probably indicating a progressive impairment of aerobic energy provision in the heart muscle. Although slightly lower in Hb-rich animals, the critical P_{O_2amb} values of the two groups were not significantly different. This was in contrast to the substantial differences found in f_A and I_{NADH} of the limb muscles, whose critical P_{O_2amb} values were significantly lower in Hb-rich than in Hb-poor animals. A possible reason for this discrepancy could lie in the positions of the respective heart and limb muscle tissues within the circulatory system. The heart is located in a more proximate position downstream of the main respiratory gas exchanger (i.e. the inner walls of the carapace; Fryer, 1991; Pirow et al., 1999b), and it receives freshly

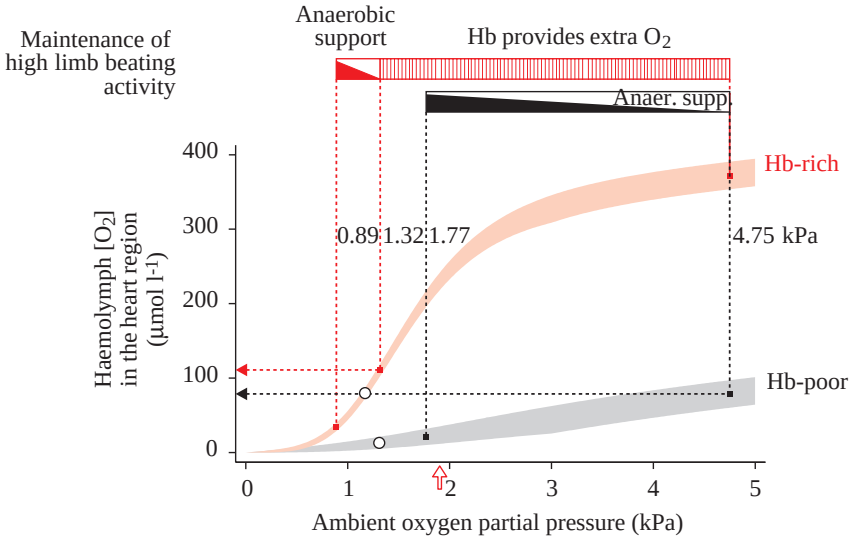

Fig. 10. Knowing their dependencies on ambient oxygen partial pressure (P_{O_2amb}) made it possible to correlate limb beating activity with haemolymph oxygen concentration ($[O_2]$). In haemoglobin (Hb)-rich animals, the physiological effect of a sevenfold higher Hb concentration manifested itself in the range of P_{O_2amb} from 4.75 to 1.32 kPa, within which the extra Hb could still provide enough oxygen to sustain aerobic energy provision in the highly active limb muscles. Within almost the same range of P_{O_2amb}, Hb-poor animals were also able to maintain a high limb beating activity, but energy provision was already supported by anaerobic mechanisms (see Fig. 8). Note that, in the two groups, anaerobic energy provision was initiated at different levels of $[O_2]$ (horizontal arrows). The open circles indicate the P_{O_2amb} and the corresponding $[O_2]$ that caused an impairment of cardiac activity. The breadth of the graphs reflects the range of uncertainty in determining the proportion of $[O_2]$ that is physically dissolved in the haemolymph. The red arrow indicates the P_{O_2amb} at which Hb-rich animals were raised.

oxygenated haemolymph (Fig. 9A). Along its way from the heart to the limbs, the haemolymph releases oxygen to other tissues, and the amount of oxygen that remains available to the proximate parts of the limb muscles, which originate on fibrous endoskeletal structures of the trunk (Binder, 1932; Fryer, 1991), is consequently lower. Hb can, if present at high concentrations, buffer this release of oxygen, and this could explain why different Hb concentrations have a clear effect on the critical P_{O_2amb} of appendage-related variables but almost none on the critical P_{O_2amb} of heart rate.

In summary, Hb-rich and Hb-poor animals showed only slight deviations in their circulatory properties such as maximum heart rate and critical P_{O_2amb}. Compared with the pronounced differences in Hb concentration, the differences in perfusion-related variables appear to be of marginal relevance in explaining the clear differences in limb beating activity.

Choosing the heart region as the location for obtaining the *in vivo* saturation curve of Hb represented a compromise. Ideally, such a measurement would be made at two locations in the circulatory system, i.e. immediately downstream of the gas exchanger and at the target tissue. This would provide information on how much oxygen enters the system and how much of this oxygen remains available to the tissue. However, in spite of the remarkable transparency of *D. magna*, which generally allows the application of optical techniques, the oxygen-saturation of Hb could be successfully determined only in peripheral haemolymph regions of the animal (Pirow et al., 1999b), but not in the vicinity of the more centrally located tissues, including the proximate parts of the appendage muscles. The heart region permitted the determination of Hb oxygen-saturation by microspectroscopy and represented the most suitable location for estimating the amount of oxygen transported into the body.

The total amount of oxygen ($\dot{M}_{O_2}$) (nmol h^{-1}) that the heart transports per hour into the body can be calculated according to the Fick principle of convection (Piiper et al., 1971):

$$\dot{M}_{O_2} = \dot{Q}[O_2], \quad (8)$$

where $\dot{Q}$ (µl h^{-1}) represents the perfusion rate and $[O_2]$ (µmol l^{-1}) is the oxygen concentration of the haemolymph in the heart region. In the haemolymph, oxygen is physically dissolved and chemically bound to haemoglobin. The following equation permits the calculation of $[O_2]$ with respect to the ambient oxygen partial pressure P_{O_2amb} (kPa):

$$[O_2](P_{O_2amb}) = \alpha_{HL}P_{O_2int} + C_{Haem}S(P_{O_2amb}), \quad (9)$$

where α_{HL} is the physical solubility of oxygen in the haemolymph [12.33 µmol l^{-1} kPa^{-1} for human plasma with 58–85 g protein l^{-1} at 20 °C (Christoforides et al., 1969)], P_{O_2int} is the oxygen partial pressure in the haemolymph (kPa), C_{Haem} is the haem-based Hb concentration (µmol l^{-1}) and $S(P_{O_2amb})$ reflects the *in vivo* saturation curve of Hb.

Values of C_{Haem} for Hb-poor and Hb-rich animals were 48.6 and 337.2 µmol l^{-1}, respectively, whereas $S(P_{O_2amb})$ was derived from the sigmoidal regression lines (Fig. 6G,H). The only unknown in equation 9 is P_{O_2int}, because it could not be measured in the present study. It is, in principle, possible to derive this variable from a comparison of the *in vivo* saturation curve with the corresponding oxygen equilibrium curve. Because of the uncertainty about what the corresponding oxygen equilibrium curve actually is, we thought it reasonable and safe to assume that P_{O_2int} lay within the range from P_{O_2amb} to P_{O_2amb}–3 kPa. This assumption is in line with the results of a recent study (C. Bäumer, personal communication) in which the oxygen partial pressure of the haemolymph was directly measured in the heart region of similar-sized Hb-poor and Hb-rich *Daphnia magna* using an oxygen-sensitive dye. In the case of P_{O_2amb}<3 kPa, P_{O_2int} was assumed to lie within the range from P_{O_2amb} to 0 kPa. This approximation was only of minor consequence for the estimation of $[O_2]$ compared with the effects of the differences in the concentration and the *in vivo* saturation curve of Hb (Fig. 10).

Comparing $[O_2]$ with appendage-related variables revealed interesting relationships (Fig. 10). The I_{NADH} signal indicated that, in Hb-poor animals, oxygen provision to the limb muscles became impeded at a critical P_{O_2amb} of 4.75 kPa. At this level, Fig. 10 provides a haemolymph $[O_2]$ in the heart region of 79±18 µmol l^{-1} (mean ± range of uncertainty, see Fig. 10). In Hb-rich animals, the same critical state occurred at 1.32 kPa, which corresponded to a $[O_2]$ of 111±8 µmol l^{-1} (mean ± range of uncertainty, see Fig. 10). This value was 42 % higher than that of Hb-poor animals. To appreciate the difference in the magnitude of the calculated $[O_2]$, we entered the data into equation 8 to determine the total amount of oxygen ($\dot{M}_{O_2}$) that the heart had transported per hour into the body at the respective critical P_{O_2amb}. The perfusion rate was obtained by multiplying heart rate by stroke volume, which was quantified according to the following procedure. On the basis of video sequences of our experimental animals, we determined the median-plane cross-sectional areas of the heart at maximum contraction (systole) and dilation (diastole). At the critical P_{O_2amb}, the diastolic areas were 0.106 mm^2 (Hb-poor) and 0.097 mm^2 (Hb-rich), whereas the systolic areas were 0.065 mm^2 (Hb-poor) and 0.054 mm^2 (Hb-rich). Taking these values and the area/volume relationships provided by Bäumer et al. (C. Bäumer , R. Pirow and R. J. Paul, in preparation), the diastolic and systolic heart volumes could be calculated, and the difference between them yielded the stroke volume. For Hb-poor and Hb-rich animals, we obtained values of 14.1 and 14.0 nl, respectively. Using these stroke volumes, the maximum heart rates of Hb-poor and Hb-rich animals (363.79 and 341.72 min^{-1}) translated into perfusion rates of 307.8 and 287.0 µl h^{-1}, respectively. Taking these perfusion rates and the two estimates for the haemolymph $[O_2]$ in the heart region (79 and 111 µmol l^{-1}) at the critical P_{O_2amb} (4.75 and 1.32 kPa), equation 8 yielded $\dot{M}_{O_2}$ values of 24 nmol h^{-1} (Hb-poor) and 32 nmol h^{-1} (Hb-rich), respectively.

To test how these values relate to the respiration rate of *D. magna*, we calculated respiration rate Y (nmol O_2 $animal^{-1}$ h^{-1}) according to the equation $Y=0.3087X^{0.95}$ (Glazier, 1991), where X is the dry body mass (µg). This equation was obtained from animals whose brood had been removed from the brood

chamber prior to the respiration measurement. This point is important insofar as eggs and early embryos, although having quite low respiration rates in comparison with the brooding mother, can make a significant contribution to total body mass (Glazier, 1991). On the basis of the carapace lengths of our experimental animals (2.20±0.16 mm, N=12), it was possible to calculate a dry mass of 117 μg using the carapace length/dry mass relationship [see (Kawabata and Urabe, 1998)] for female *D. magna* without eggs or embryos in the brood chamber. On the basis of this dry mass estimate, we obtained a respiration rate of 28 nmol O_2 animal^{-1} h^{-1}.

Comparing this reference value with $\dot{M}_{O_2}$ revealed important information concerning the oxygen-transport capacity of the circulatory system of our experimental animals. At the critical P_{O_2amb} of 4.75 kPa, the hearts of Hb-poor animals transported a total of approximately 24 nmol O_2 h^{-1} into the body, a value somewhat lower than the estimated respiration rate. In contrast, Hb-rich animals were able to transport 32 nmol O_2 h^{-1} at the far lower critical P_{O_2amb} of 1.32 kPa. This value was higher than the value of Hb-poor animals and also higher than the estimated respiration rate of 28 nmol O_2 animal^{-1} h^{-1}. In spite of the fact that not all the oxygen entering the body can be utilized and that this residual amount of unused oxygen is certainly greater in Hb-rich animals because of the higher oxygen-binding affinity of Hb, it is nevertheless very likely that the circulatory system of Hb-rich animals transported a greater proportion of oxygen respired than that of Hb-poor animals.

This assumption gains support when taking the differences in the critical P_{O_2amb} into account. At the higher critical P_{O_2amb} of 4.75 kPa, Hb-poor animals can rely to a greater extent on diffusion for providing peripheral body tissues with oxygen directly from the ambient medium. This mode of oxygen transport is relevant to, for example, the epithelial tissue and the distal parts of the appendage muscles. Only the more centrally located body tissues, which are too distant from the periphery to be adequately supplied by diffusion, require a convective provision of oxygen, which is achieved by haemolymph circulation. At the far lower critical P_{O_2amb} of 1.32 kPa, the driving force for diffusion, and consequently the penetration depth of oxygen into the body, is considerably reduced. Therefore, Hb-rich animals have to rely to a greater extent on a convective supply of oxygen to the tissues, which is ensured by the Hb-mediated increase in the oxygen-transport capacity of the circulatory system.

In conclusion, the possession of a particular Hb concentration in the water flea *Daphnia magna* can be regarded as a trade-off between a desirable high tolerance for hypoxia and an equally desirable low cost of protein synthesis combined with a low visibility to predators. The synthesis of Hb seems to be useful only under conditions of reduced oxygen availability, because Hb then makes a substantial contribution to convective oxygen transport in the haemolymph, which can offset any disadvantages. In the present study, a sevenfold increase in haemolymph Hb concentration was found to effect a reduction in critical P_{O_2amb} from 4.75 to 1.32 kPa. These critical P_{O_2amb} values, at which the I_{NADH} signal indicated an impairment of the oxygen supply to the limb muscles, agreed with results for oxygen consumption and lactate production (Kobayashi and Hoshi, 1984; Usuki and Yamagushi, 1979). During chronic exposure to hypoxia (e.g. <2 kPa), the physiological benefit of Hb can therefore translate into a significant ecological advantage since it enables the organism to sustain its aerobic metabolism as the energetically most efficient mode of fuel utilization.

For future experiments, it would be interesting to determine how other cladoceran species make use of Hb and how they differ in the physiological properties they have evolved as a consequence of their adaptive radiation into a wide range of marine and freshwater habitats from polar to tropical regions (Hebert et al., 1999).

List of symbols

$A(\lambda)$	absorption spectrum
$A'(\lambda)$	corrected absorption spectrum
$A_p(\lambda)$, $A_r(\lambda)$	absorption spectra of Hb-poor and Hb-rich animals
b	absorption-related coefficient (non-Hb components)
c, d	regression coefficients
C_{Haem}	haem-based Hb concentration (μmol l^{-1})
C_p, C_r	relative Hb concentration of Hb-poor and Hb-rich animals
f_A	appendage beating rate (min^{-1})
f_H	heart rate (min^{-1})
$H(\lambda)$	Hb absorption spectra of unknown oxygen-saturation
$H_o(\lambda)$, $H_d(\lambda)$	absorption spectra of oxy-Hb and deoxy-Hb
$I(\lambda)$	intensity spectrum
$I_0(\lambda)$	reference intensity spectrum
I_{NADH}	NADH fluorescence intensity
k_0, k_1	regression coefficients
$\dot{M}_{O_2}$	rate of oxygen transport (nmol h^{-1})
n	Hill coefficient
$[O_2]$	oxygen concentration in the haemolymph (μmol l^{-1})
P_{O_2}	oxygen partial pressure (kPa)
P_{O_2amb}	ambient oxygen partial pressure (kPa)
P_{O_2int}	oxygen partial pressure in the haemolymph (kPa)
P_{50}	oxygen partial pressure at which Hb is half-saturated (kPa)
$\dot{Q}$	perfusion rate (μl h^{-1})
S	oxygen-saturation coefficient
$S(P_{O_2amb})$	*in vivo* saturation curve of Hb
X	dry body mass (μg)
Y	respiration rate (nmol O_2 animal^{-1} h^{-1})
α,β	absorption bands of oxy-Hb
α_{HL}	physical solubility for oxygen in the haemolymph (μmol l^{-1} kPa^{-1})
λ	wavelength (nm)

The technical assistance of Ina Buchen is gratefully acknowledged. We especially thank Alan Rietmann Knauth for the linguistic and stylistic improvements to the manuscript. Helpful comments on the manuscript were provided by two anonymous reviewers. Supported by the Deutsche Forschungsgemeinschaft (Pa 308/7-1).

References

Antonini, E. and Brunori, M. (1971). Hemoglobin and myoglobin in their reactions with ligands. *Frontiers in Biology Series*, vol. 21. 436p. Amsterdam, London: North-Holland Publishing Company.

Binder, G. (1932). Das Muskelsystem von *Daphnia*. *Int. Rev. Ges. Hydrobiol. Hydrog.* **26**, 54–111.

Bohrer, R. N. and Lampert, W. (1988). Simultaneous measurement of the effect of food concentration on assimilation and respiration in *Daphnia magna* Straus. *Funct. Ecol.* **2**, 463–471.

Brönmark, C. and Hansson, L.-A. (1998). *The Biology of Lakes and Ponds*. Oxford, New York, Tokyo: Oxford University Press.

Carvalho, G. R. (1984). Haemoglobin synthesis in *Daphnia magna* Straus (Crustacea: Cladocera): ecological differentiation between neighbouring populations. *Freshwater Biol.* **14**, 501–506.

Chance, B. (1991). Optical method. *Annu. Rev. Biophys. Chem.* **20**, 1–28.

Chandler, A. (1954). Causes of variation in the haemoglobin content of *Daphnia* (Crustacea: Cladocera). *Proc. Zool. Soc. Lond.* **124**, 625–630.

Christoforides, C., Laasberg, L. H. and Hedley-Whyte, J. (1969). Effect of temperature on solubility of O_2 in human plasma. *J. Appl. Physiol.* **26**, 56–60.

Confer, J. L., Howick, G. L., Corzette, M. H., Kramer, S. L., Fitzgibbon, S. and Landesberg, R. (1978). Visual predation by planktivores. *Oikos* **31**, 27–37.

Dresel, E. I. B. (1948). Passage of haemoglobin from blood into eggs of *Daphnia*. *Nature* **162**, 736–737.

Elendt, B.-P. and Bias, W.-R. (1990). Trace nutrient deficiency in *Daphnia magna* cultured in standard medium for toxicity testing. Effects of the optimization of culture conditions on life history parameters of *D. magna*. *Water Res. Biol.* **24**, 1157–1167.

Flößner, D. (1972). Krebstiere, Crustacea: Kiemen- und Blattfüßer, Branchiopoda; Fischläuse, Branchiura. In *Die Tierwelt Deutschlands* (ed. M. Dahl and F. Peus), part 60. Jena: Gustav Fischer.

Fox, H. M. (1948). The haemoglobin of *Daphnia*. *Proc. R. Soc. B* **135**, 195–212.

Fox, H. M. (1955). The effect of oxygen on the concentration of haem in invertebrates. *Proc. R. Soc. B* **143**, 203–214.

Fox, H. M., Gilchrist, B. M. and Phear, E. A. (1951). Functions of haemoglobin in *Daphnia*. *Proc. R. Soc. B* **138**, 514–528.

Fox, H. M., Hardcastle, S. M. and Dresel, E. I. B. (1949). Fluctuations in the haemoglobin content of *Daphnia*. *Proc. R. Soc. B* **136**, 388–399.

Fox, H. M. and Phear, E. A. (1953). Factors influencing haemoglobin synthesis by *Daphnia*. *Proc. R. Soc. B* **141**, 179–189.

Freitag, J. F., Steeger, H.-U., Storz, U. C. and Paul, R. J. (1998). Sublethal impairment of respiratory control in plaice (*Pleuronectes platessa*) larvae induced by UV-B radiation, determined using a novel biocybernetical approach. *Mar. Biol.* **132**, 1–8.

Fritzsche, H. (1917). Studien über Schwankungen des osmotischen Druckes der Körperflüssigkeiten bei *Daphnia magna*. *Int. Rev. Ges. Hydrobiol. Hydrog.* **8**, 22–80.

Fryer, G. (1991). Functional morphology and the adaptive radiation of the Daphniidae (Branchiopoda: Anomopoda). *Phil. Trans. R. Soc. Lond. B* **331**, 1–99.

Fryer, G. (1996). Diapause, a potent force in the evolution of freshwater crustaceans. *Hydrobiol.* **320**, 1–14.

Glazier, D. S. (1991). Separating the respiration rates of embryos and brooding females of *Daphnia magna*: Implications for the cost of brooding and the allometry of metabolic rate. *Limnol. Oceanogr.* **36**, 354–362.

Green, J. (1955). Studies on a population of *Daphnia magna*. *J. Anim. Ecol.* **24**, 84–97.

Green, J. (1956). Variations in the haemoglobin content of *Daphnia*. *Proc. R. Soc. Lond.* **145**, 214–232.

Green, J. (1956). Growth, size and reproduction in *Daphnia* (Crustacea: Cladocera). *Proc. Zool. Soc. Lond.* **126**, 173–204.

Hebert, P. D. N., Um, Y. M., Prokopowich, C. D. and Taylor, D. J. (1999). Gene conversion and evolution of daphniid hemoglobins (Crustacea, Cladocera). *J. Mol. Evol.* **49**, 769–779.

Heisey, D. and Porter, K. G. (1977). The effect of ambient oxygen concentration on filtering rate and respiration rate of *Daphnia magna mendotae* and *Daphnia magna*. *Limnol. Oceanogr.* **22**, 839–845.

Herreid, C. F. (1980). Hypoxia in invertebrates. *Comp. Biochem. Physiol.* **67A**, 311–320.

Hoshi, T. and Kobayashi, M. (1971). Studies on physiology and ecology of plankton. XXV. Iron-content and millimolar extinction coefficient of the *Daphnia*-haemoglobin. *Sci. Rep. Niigata Univ. Ser. D (Biol.)* **8**, 65–68.

Hoshi, T. and Yahagi, N. (1975). Studies on physiology and ecology of plankton. XXIX. *In vivo* equilibrium of oxygen with blood haemoglobin of *Daphnia magna*. *Sci. Rep. Niigata Univ. Ser. D (Biol.)* **12**, 1–7.

Jones, J. D. (1972). *Comparative Physiology of Respiration. Special Topics in Biology Series.* London: Edward Arnold.

Kawabata, K. and Urabe, J. (1998). Length–weight relationships of eight freshwater planktonic crustacean species in Japan. *Freshwater Biol.* **39**, 199–205.

Kimura, S., Tokishita, S., Ohta, T., Kobayashi, M. and Yamagata, H. (1999). Heterogeneity and differential expression under hypoxia of two-domain hemoglobin chains in the water flea, *Daphnia magna*. *J. Biol. Chem.* **274**, 10649–10653.

Kobayashi, M. (1981). Influences of haemoglobin concentration and temperature on oxygen uptake of *Daphnia magna* under low oxygen concentration. *Comp. Biochem. Physiol.* **69A**, 679–682.

Kobayashi, M. (1982). Influence of body size on haemoglobin concentration and resistance to oxygen deficiency in *Daphnia magna*. *Comp. Biochem. Physiol.* **72A**, 599–602.

Kobayashi, M., Fujiki, M. and Suzuki, T. (1988). Variation in and oxygen-binding properties of *Daphnia magna* hemoglobin. *Physiol. Zool.* **61**, 415–419.

Kobayashi, M. and Gonoi, T. (1985). Horizontal movement of pale and red *Daphnia magna* in low oxygen concentration. *Physiol. Zool.* **58**, 190–196.

Kobayashi, M. and Hoshi, T. (1982). Relationship between the haemoglobin concentration of *Daphnia magna* and the ambient oxygen concentration. *Comp. Biochem. Physiol.* **72A**, 247–249.

Kobayashi, M. and Hoshi, T. (1984). Analysis of respiratory role of haemoglobin in *Daphnia magna*. *Zool. Sci.* **1**, 523–532.

Kobayashi, M., Kato, S., Ninomiya, M., Fujiki, M., Igarashi, Y. and Kajita, A. (1990a). Hemoglobin in the parthenogenetic eggs of *Daphnia magna*. *J. Exp. Zool.* **254**, 18–24.

Kobayashi, M. and Nezu, T. (1986). Variation in hemoglobin content in *Daphnia magna*. *Physiol. Zool.* **59**, 35–42.

Kobayashi, M., Nezu, T. and Tanaka, Y. (1990b). Hypoxic induction of hemoglobin synthesis in *Daphnia magna*. *Comp. Biochem. Physiol.* **97A**, 513–517.

Kobayashi, M. and Tanaka, Y. (1991). Oxygen-transporting function of hemoglobin in *Daphnia magna*. *Can. J. Zool.* **69**, 2968–2972.

Kring, R. L. and O'Brien, W. J. (1976). Effect of varying oxygen concentrations on the filtering rate of *Daphnia pulex*. *Ecology* **57**, 808–814.

Lampert, W. (1986). Response of the respiratory rate of *Daphnia magna* to changing food conditions. *Oecologia* **70**, 495–501.

Lampert, W. (1989). The adaptive significance of diel vertical migration. *Funct. Ecol.* **3**, 21–27.

Lampert, W. (1993). Ultimate causes of diel vertical migration of zooplankton: New evidence for the predator-avoidance hypothesis. *Arch. Hydrobiol. Beih. Ergebn. Limnol.* **39**, 79–88.

Meijering, M. P. D. (1958). Herzfrequenz und Lebenslauf von *Daphnia magna* Straus. *Z. Wiss. Zool.* **161**, 239–265.

O'Brien, W. J. (1979). The predator–prey interaction of planktivorous fish and zooplankton. *Am. Sci.* **67**, 572–581.

Paul, R. J., Colmorgen, M., Hüller, S., Tyroller, F. and Zinkler, D. (1997). Circulation and respiratory control in millimetre-sized animals (*Daphnia magna*, *Folsomia candida*) studied by optical methods. *J. Comp. Physiol. B* **167**, 399–408.

Paul, R. J., Colmorgen, M., Pirow, R., Chen, Y.-H. and Tsai, M.-C. (1998). Systemic and metabolic responses in *Daphnia magna* to anoxia. *Comp. Biochem. Physiol.* **120A**, 519–530.

Paul, R. J., Gohla, J., Föll, R. and Schneckenburger, H. (2000). Metabolic adaptations to environmental changes in *Caenorhabditis elegans*. *Comp. Biochem. Physiol.* **127B**, 469–479.

Piiper, J., Dejours, P., Haab, P. and Rahn, H. (1971). Concepts and basic quantities in gas exchange physiology. *Respir. Physiol.* **13**, 292–304.

Pirow, R., Wollinger, F. and Paul, R. J. (1999a). Importance of the feeding current for oxygen uptake in the water flea *Daphnia magna*. *J. Exp. Biol.* **202**, 553–562.

Pirow, R., Wollinger, F. and Paul, R. J. (1999b). The sites of respiratory gas exchange in the planktonic crustacean *Daphnia magna*: an *in vivo* study employing blood haemoglobin as an internal oxygen probe. *J. Exp. Biol.* **202**, 3089–3099.

Press, W. H., Teukolsky, S. A., Vetterling, W. T. and Flannery, B. P. (1992). *Numerical Recipes in C*. Cambridge: Cambridge University Press.

Prosser, C. L. and Brown, F. A., Jr (1961). *Comparative Animal Physiology*. Philadelphia: Saunders.

Randall, D., Burggren, W. and French, K. (1997). *Eckert Animal Physiology: Mechanisms and Adaptations*. New York: W. H. Freeman & Company.

Sell, A. F. (1998). Adaptation to oxygen deficiency: Contrasting patterns of haemoglobin synthesis in two coexisting *Daphnia* species. *Comp. Biochem. Physiol.* **120A**, 119–125.

Sugano, H. and Hoshi, T. (1971). Purification and properties of blood hemoglobin from fresh-water cladocera, *Moina macropa* and *Daphnia magna*. *Biochim. Biophys. Acta* **229**, 349–358.

Terwilliger, N. B. (1998). Functional adaptations of oxygen-transport proteins. *J. Exp. Biol.* **201**, 1085–1098.

Terwilliger, R. C. (1980). Structure of invertebrate hemoglobins. *Am. Zool.* **20**, 53–67.

Tokishita, S., Shiga, Y., Kimura, S., Ohta, T., Kobayashi, M., Hanazoto, T. and Yamagata, H. (1997). Cloning and analysis of a cDNA encoding a two-domain hemoglobin chain from the water flea *Daphnia magna*. *Gene* **189**, 73–78.

Usuki, I. and Yamagushi, K. (1979). Physiological significance of the extracellular haemoglobin on the survival and lactic acid production of *Daphnia magna* Straus in low oxygen conditions. *Sci. Rep. Niigata Univ. Ser. D (Biol.)* **16**, 5–12.

Vinogradov, S. N. (1985). The structure of invertebrate extracellular hemoglobins (erythrocruorins and chlorocruorins). *Comp. Biochem. Physiol.* **82B**, 1–15.

Vinyard, G. L. and O'Brien, W. J. (1975). Dorsal light response as an index of prey preference in bluegill sunfish (*Lepomis macrochirus*). *J. Fish. Res. Bd Can.* **32**, 1860–1863.

Wakita, M., Nishimura, G. and Tamura, M. (1995). Some characteristics of the fluorescence lifetime of reduced pyridine nucleotides in isolated mitochondria, isolated hepatocytes and perfused rat liver *in situ*. *J. Biochem.* **118**, 1151–1160.

Weber, R. E. (1980). Functions of invertebrate hemoglobins with special reference to adaptations to environmental hypoxia. *Am. Zool.* **20**, 79–101.

Weider, L. J. (1985). Spatial and temporal genetic heterogeneity in a natural *Daphnia* population. *J. Plankton Res.* **7**, 101–123.

Weider, L. J. and Lampert, W. (1985). Differential response of *Daphnia* genotypes to oxygen stress: respiration rates, hemoglobin content and low-oxygen tolerance. *Oecologia* **65**, 487–491.

Williamson, C. E., Sanders, R. W., Moeller, R. E. and Stutzman, P. L. (1996). Utilization of subsurface food resources for zooplankton reproduction: Implications for diel vertical migration theory. *Limnol. Oceanogr.* **41**, 224–233.